PROCEEDINGS OF SPIE

SPIEDigitalLibrary.org/conference-proceedings-of-spie

Multi-angle VECSEL cavities for dispersion control and multi-color operation

Caleb Baker
Maik Scheller
Alexandre Laurain
Hwang-Jye Yang
Antje Ruiz Perez
Wolfgang Stolz
Sadhvikas J. Addamane
Ganesh Balakrishnan
R. Jason Jones
Jerome V. Moloney

SPIE.

Multi-angle VECSEL cavities for dispersion control and multi-color operation.

Caleb Baker*[a], Maik Scheller[a], Alexandre Laurain[a], Hwang-Jye Yang[a], Antje Ruiz Perez[b], Wolfgang Stolz[b], Sadhvikas J. Addamane[c], Ganesh Balakrishnan[c], R. Jason Jones[a], Jerome V. Moloney[a]

[a]College of Optical Sciences, The University of Arizona, 1630 E University Blvd, Tucson, AZ, US 85719; [b]Fachbereich Physik, Philipps-Universitat Marburg, Renthof 5, D-35032 Marburg, Germany; [c]ECE Dept. Center for High Technology Materials, University of New Mexico, 1313 Goddard SE, Albuquerque, NM, US 87106-4343

Abstract

We present a novel Vertical External Cavity Surface Emitting Laser (VECSEL) cavity design which makes use of multiple interactions with the gain region under different angles of incidence in a single round trip. This design allows for optimization of the net, round-trip Group Delay Dispersion (GDD) by shifting the GDD of the gain via cavity fold angle while still maintaining the high gain of resonant structures. The effectiveness of this scheme is demonstrated with femtosecond-regime pulses from a resonant structure and record pulse energies for the VECSEL gain medium. In addition, we show that the interference pattern of the intracavity mode within the active region, resulting from the double-angle multifold, is advantageous for operating the laser in CW on multiple wavelengths simultaneously. Power, noise, and mode competition characterization is presented.

Keywords: VECSEL, Ultrafast, 2-color, F-cavity

1. INTRODUCTION

VECSELs are an emergent class of semiconductor laser currently undergoing significant efforts to be generalized into the ultrafast regime. The promise of the VECSEL medium has been well demonstrated with continuous wave (CW) emission exceeding 100W [1], great wavelength flexibility at the design stage [2,3], and external cavities which allow for filtering or frequency doubling elements to be included intracavity [4,5]. Efforts to modelock VECSELs have yielded pulses below 100fs [6] and operation in the kilowatt range of peak powers [7,8]. Multi-color operation has also been demonstrated in VECSELs both in CW [9] and pulsed [10] operation.

Use of long (>10-15cm) cavities in VECSEL designs is common, but is often limited when modelocking VECSELs by the medium's nanosecond upper state lifetime. Because of this, cavities which make multiple passes through the gain are often used when constructing pulsed VECSELs with repetition rates in the hundreds of MHz or lower [11,12]. In this paper we present a novel multi-pass cavity design that contains two arms interacting with the gain under different angles. The use to two significantly different angles results in two features which we present in their own sections below. First, the Group Delay Dispersion (GDD) profile of the gain will blue shift with increasing angle, allowing potential compensation of GDD resonances often seen in devices grown for high gain. Second, the two angles prompt an interference pattern where the intracavity field interacts with the active region; this pattern possesses sharp intensity spikes with a wavelength-dependent separation, allowing for decreased mode overlap (and thus, decreased gain competition) in the outer regions of the spatial modes of two nm-separated lasing wavelengths.

The primary results we present are a modelocked VECSEL emitting pulses with 6.3 kW of peak power (section 2) and a highly stable CW emission of 2.6 W on two wavelengths with a 1.0 THz separation (section 3).

*cwbaker@email.arizona.edu

Vertical External Cavity Surface Emitting Lasers (VECSELs) VII, edited by Michael Jetter, Proc. of SPIE Vol. 10087, 100870B · © 2017 SPIE · CCC code: 0277-786X/17/$18 · doi: 10.1117/12.2250579

2. MODELOCKING

2.1 Modelocking Introduction

Designing VECSELs for modelocked operation presents several challenges. The typical structure of a high-power CW VECSEL, as in [1], possesses several characteristics that are disadvantageous to modelocked operation. The microcavity formed by the Distributed Bragg Reflector (DBR) and the surface layer serves as a low-Q fabry-perot etalon, and thus can impose a spectral filter, limiting the lasing bandwidth. The placement of the quantum wells, being strongly resonant with a particular target wavelength, can also limit the spectral broadness. Both of these effects contribute to maximizing the field enhancement factor for a narrow spectrum interacting with the gain. At maximum field enhancement, the lasing mode burns a deep, narrow hole in the carrier distribution, allowing for nonequilibrium effects such as kinetic hole burning to influence pulse formation [13].

One of the most common methods of designing VECSELs for modelocked operation is to apply an anti-reflection coating to the surface of the device. These coatings can range from a simple 1-2 layers (see [14] as an example) to much more intricate designs (e.g. [6]) and serve to both reduce the filtering effect of the device's microcavity and control the device's GDD to flat and near-zero within the lasing band. In addition, it has been shown that precisely etching the surface layer of the device can function similarly to an AR coating and give similar results [7]. Work surrounding the shortest pulses observed in VECSELs has shown that reducing the number of quantum wells in the active region [15] and/or placing quantum wells in careful positions off of the target wavelength's standing wave antinodes can greatly improve modelocking performance [6, 13]. Both of these strategies lower the gain – and thus the potential power scalability – of the device, but support broader lasing spectra and limit the influence of non-equilibrium effects.

Because obtaining the shortest pulses have so far been done by lowering the gain of a VECSEL significantly, more standard RPG designs remain the holders of record peak powers [7]. We present here another method of controlling the dispersion of these devices, as their potential for high power scalability without external amplifiers is still attractive. We note that the dispersion profiles of these devices typically possess a resonance feature with positive and negative extrema. This resonance feature blue shifts as the angle of incidence between the lasing mode and the device increases, allowing for two passes through the gain at strongly differing angles to present dramatically different dispersion profiles. The goal of our multi-fold cavity (F-cavity) design is for this shift to result in the two different passes having a compensatory effect on each others' GDD within the lasing band.

2.2 Experimental setup

The VECSEL we use was grown on a GaAs substrate and possesses an AlGaAs-GaAs DBR, an active region with ten InGaAs quantum wells placed resonantly between GaAsP barriers, an InGaP cap layer, and a single-layer SiN AR coating. A diamond heat spreader is soldered to the back of the DBR to assist in heat extraction and the device is placed on a water-cooled mount inside the cavity as seen in Fig 1. It is pumped with an 808nm fiber-coupled diode bar and was designed to emit at around 1040nm.

The F-cavity itself is 38 cm long (390 MHz), but has no arm with a travel time approaching the nanosecond time scales of the VECSEL's carrier lifetimes. The narrow and wide folds are 10° and 40°, respectively, the output coupling is 3%, and all elements were measured to have negligible GDD within the lasing band except for the VECSEL and Semiconductor Saturable Absorber (SESAM). The spot size ratio between the SESAM and VECSEL is a fairly standard 1/2 and the separate passes through the gain were very precisely aligned to exactly overlap within the pumped gain region.

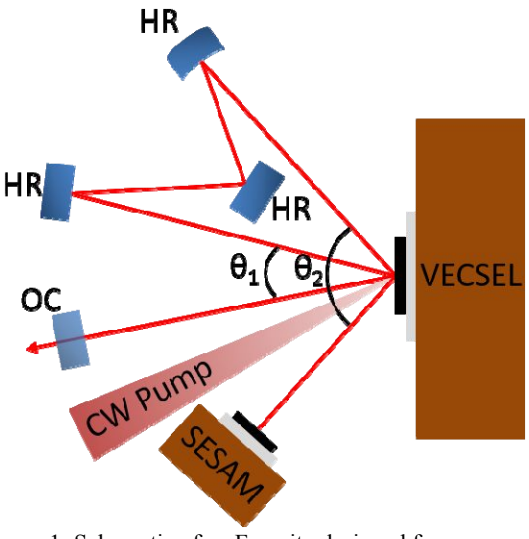

Figure 1: Schematic of an F-cavity designed for modelocking.

2.3 Modelocking Results

Modelocking was observed in this configuration between 7W and 12W of pump power, with little variation in pulse shape or behavior. Above 12W of pump, the modelocking state grew increasingly unstable. We suspect that the high intracavity field due to the multi-pass design oversaturating the SESAM was the primary cause, allowing for the potential of further power scaling if a higher saturation fluence SESAM were used.

The optimal peak power was obtained at 12 W, corresponding to an average output power of 1.14W. Fig. 2 shows the 410 fs pulse with a secant shape and (inset) the corresponding 3.2 nm spectrum. Fig 3 shows the fundamental peak of the recorded RF spectrum at 390MHz (limited by a resolution bandwidth of 1 kHz) and (inset) a lower resolution scan including the first harmonic, to demonstrate the existence of stable, single-pulse, modelocked operation. With these

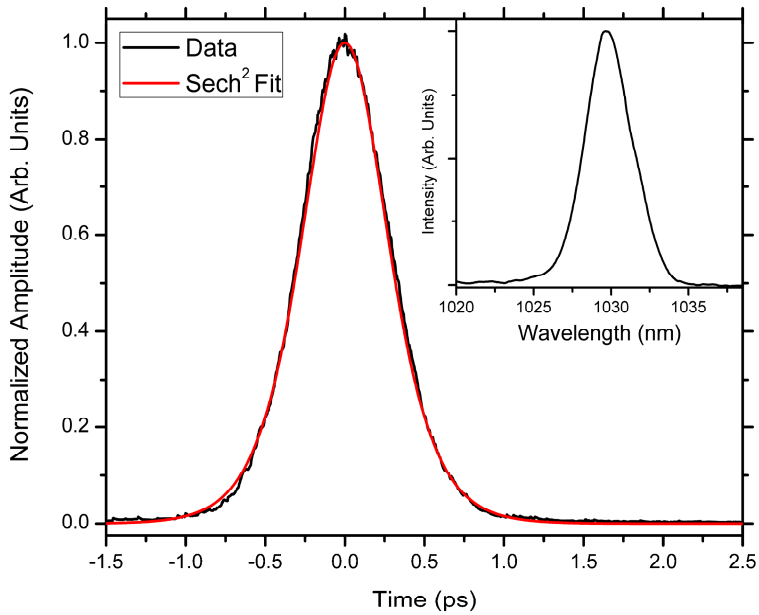

Figure 2: Autocorrelation of 410 fs pulse with (inset) corresponding 3nm spectrum.

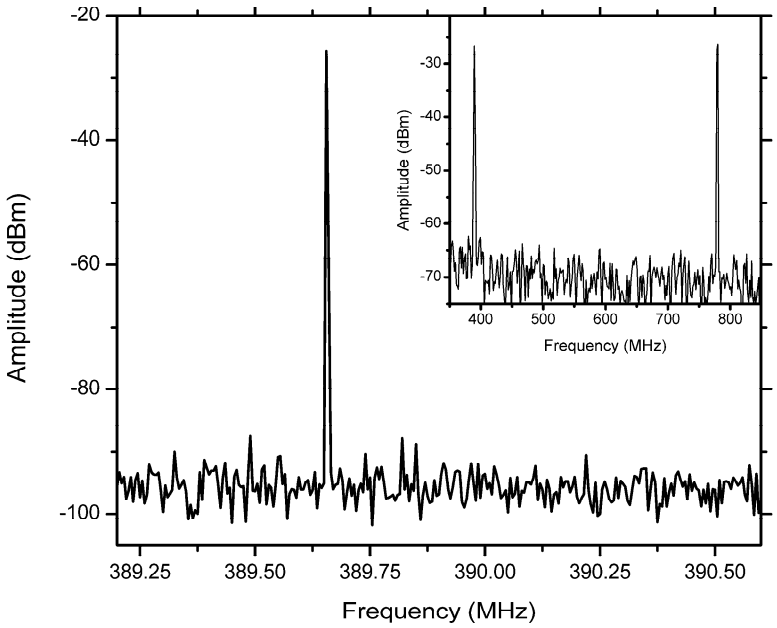

Figure 3: Recorded RF spectrum displaying narrow linewidth and (inset) lower resolution displaying first and second harmonics of the RF peak..

parameters, and assuming a secant-shaped pulse, we calculate a record peak power of 6.3 kW.

2.4 Modelocking Discussion

In order to show that the dispersion-shifting properties of our cavity are specifically what led to the results above, we first tested the same chip in a more standard V-cavity. We used a 10cm V-cavity with a standard ~1/3 mode ratio and lowered the output coupling to 1% to adjust for the lower intracavity powers as the cavity was not multi-pass. We recorded >1ps pulses after optimizing heatsink temperatures for shortest pulse duration.

We then noted that the shifting of interaction parameters with angle of incidence should also be polarization dependent; the cavity's TE and TM polarizations should shift different. A thin (~100 micron) glass etalon placed at Brewster's angle for either of these polarizations was used as a polarization filter – imposing heavy losses to the one polarization while providing negligible loss, GDD, and spectral filtering to the other. Very careful attention was paid to ensuring the glass Brewster window was indeed at Brewster's angle and we found that when it supported the cavity's TE polarization, the results in section 2.3 were attained. However, when the Brewster window was rotated to support the cavity's TM polarization, the shortest pulses we could attain were ~16ps. The two different pulses are displayed in Fig. 4.

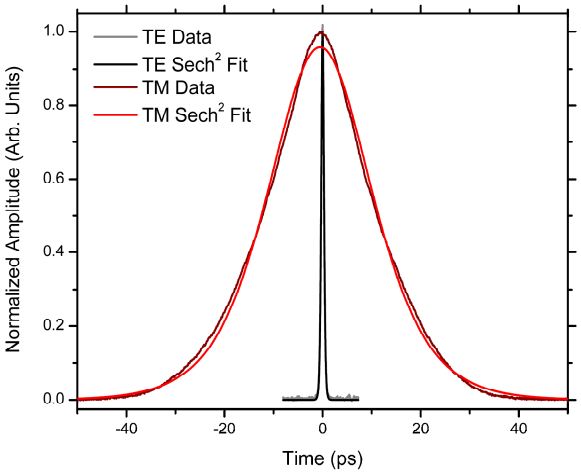

Figure 4: Pulse width comparison between operation when the cavity TE mode is enforced (black; see Fig 2 for zoom) and when its TM mode is enforced (red).

To better understand the mechanics of these results, we use a transfer matrix method to simulate the GDD of the VECSEL under lasing conditions. To start, a white light interferometer was used to measure the room temperature, normal-incidence GDD of both the VECSEL and SESAM with a resolution of +/- 5 fs^2 and a calibrated white light source was used to measure the room temperature reflectivity of the VECSEL. Then, the layer thicknesses and material composition were adjusted in the simulation so that the simulated GDD and reflectivity precisely matched the measurements. Finally, the temperature and carrier density were then estimated according to [16] and the simulation parameters were adjusted to those estimates.

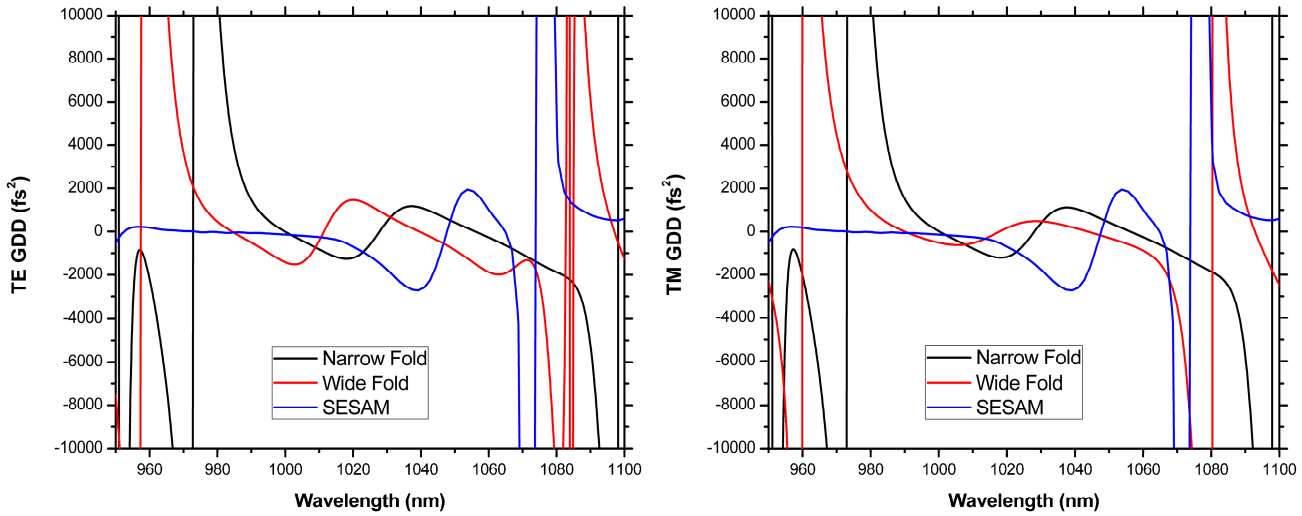

Figure 5: Simulation of single pass GDD in our VECSEL for narrow (black) and wide (red) angles, for both cavity TE mode (left) and cavity TM mode (right). Measured SESAM GDD (blue) is included in both for reference.

Fig. 5 displays the simulated VECSEL GDD for TE and TM modes of the cavity alongside the SESAM GDD. Additionally, Fig. 6 shows the net cavity GDD, two passes through each angle of the simulated VECSEL GDD and one pass through the SESAM GDD. It is clear to see that for the TM mode, the round-trip GDD profile deviates significantly from the ideal profile of flat and near-zero. For the TE mode, however, the negative slopes of the wide angle fold and the SESAM compensate for the positive slope of the narrow-angle fold and yield a net GDD that is relatively flat and slightly positive within the marked lasing bandwidth.

This agrees very well with the experimental data, where enforcing the cavity TE mode yielded 410 fs pulses while enforcing the cavity TM mode produced pulses over 16 ps. These results indicate that managing the GDD of a modelocked VECSEL through angle of incidence tuning is a practical strategy.

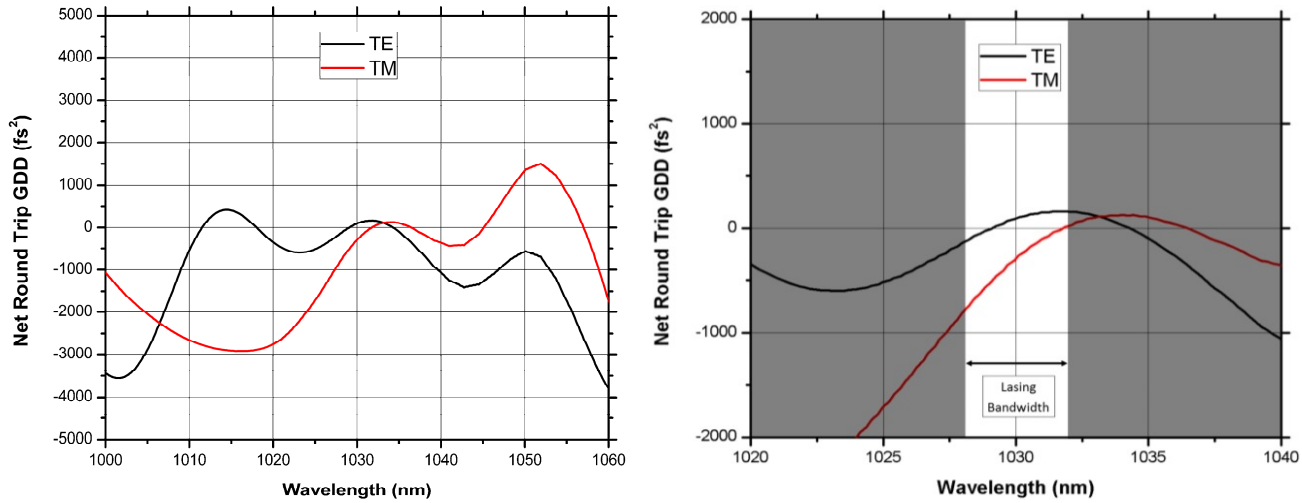

Figure 6: Simulated net roundtrip GDD for our VECSEL chip in our F-cavity design for cavity TE (black) and TM (red) modes. (Right) Zoom of this data displaying relevant details to the highlighted lasing bandwidth.

3. 2-COLOR OPERATION

3.1 2-Color Introduction

It has been previously shown that kinetic hole burning in the excited carrier population of VECSEL quantum wells allows for emission on multiple wavelengths at the same time [17,18]. Experimental investigations have shown that for high intracavity powers, relatively stable coexistence of two wavelengths is possible [9,19], but at lower intracavity intensities, a strong anti-correlation noise is present due to mode competition between the two colors. Because high output powers typically require high output coupling, reducing intracavity powers, finding a way to mitigate this mode competition would greatly improve the potential of VECSELs as 2-color sources for applications such as difference frequency generation (DFG) of terahertz.

Here, we investigate the effectiveness of the F-cavity with regard to multi-wavelength emission. The two folds under significantly different angles provide a unique interference pattern with sharp intensity spikes. Because the distribution of this interference is wavelength dependent, partial decoupling of the spatial overlap between the two modes is possible and since each mode will burn a spatial hole according to its fringe pattern, gain competition can be alleviated. We present data for two wavelengths spaced by 1 THz and compare the device's power and stability to a conventional single pass cavity.

3.2 2-Color Setup

The F-cavity setup is nearly identical to the setup in section 2, however the SESAM has been removed in favor of an HR mirror. The comparison cavity is a V-cavity configuration where the VECSEL is placed as end mirror and a 1% output coupling is again used in lieu of the multi-pass cavity's 3% in order to keep the intracavity powers high despite there being fewer passes through the gain. To induce 2-color emission, we employ the same etalon used in the polarization enforcement discussion in section 2.4, but now it is not used at Brewster's angle as spectral filtering is desirable for controlling the lasing bandwidth(s). The etalon's free spectral range is 1 THz.

In order to measure the anti-phase noise in the powers of the emitted wavelengths, and thus observe the magnitude of the gain competition between the two lasing modes, we employ a grating to spatially separate the wavelengths and then guide each beam to a fast photodetector (100 MHz bandwidth). This allows for fast simultaneous detection of each of the emitted lasing bandwidths.

Lastly, to ensure a good comparison between the two cavities, we align them to the same spot on the VECSEL chip such that either can lase if allowed. We then employ a beam stop to select the operational cavity by completely blocking one arm of its counterpart. This allows us to keep the gain region used consistent without potential errors in the alignment process.

3.3 2-Color Results

Fig. 7 shows a power curve for the two cavities investigated. While the curve displays a maximum power for the F-cavity of over 3W without reaching rollover, the maximum power achieved with nearly equal distribution between the two lasing bands was 2.6 W. The V-cavity, by comparison, displays a maximum output power of 1.3W. With 3% and

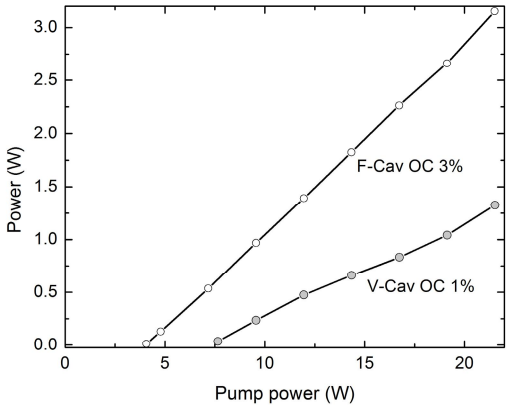

Figure 7: Power curves for F-cavity and comparison V-cavity. 2-color operation was stable for most of the F-cavity portion of this curve, but the maximum power with equal power in both modes was 2.6W.

1% output couplings for the F- and V-cavities, respectively, these output powers correspond to intracavity powers of below 100W – quite low compared to the stability range observed in [19].

Fig. 8 shows the time dynamics of the two lasing wavelengths, as measured on separate fast photodiodes, in comparison between the two cavity setups. As one can see, the V-cavity exhibits a strong anti-correlated noise between the two wavelengths as strong mode competition is present. Meanwhile the F-cavity exhibits highly stable 2-color operation with small amounts of anti-correlation noise. Further, Fig. 9 shows the operational regime of the pump laser under which these two cavities emit stable 2-color ("stable" meaning that there are no prolonged periods where either mode "wins" and is the sole lasing mode). The error bars indicate the magnitude of the mode competition shown by example in Fig. 9. The difference in stability regime relative to pump power slightly exceeds a factor of 5 between the two cavities and even at each level of operation, the multi-pass design exhibits very low noise relative to the V-cavity comparison. Further, the increased operational range in terms of pump power could also assist in longer temporal stability as the F-

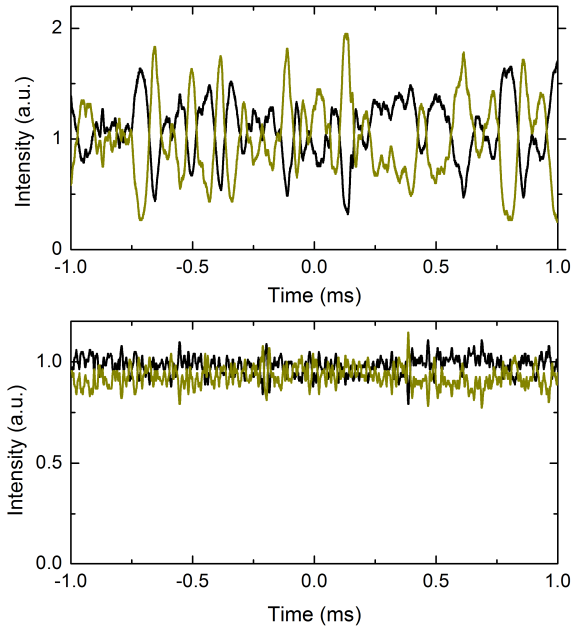

Figure 8: Fast photodiode readings of the two lasing bands for V-cavity (top) and F-cavity (bottom). The magnitude of the anti-correlation noise is indicative of the competition between the two modes.

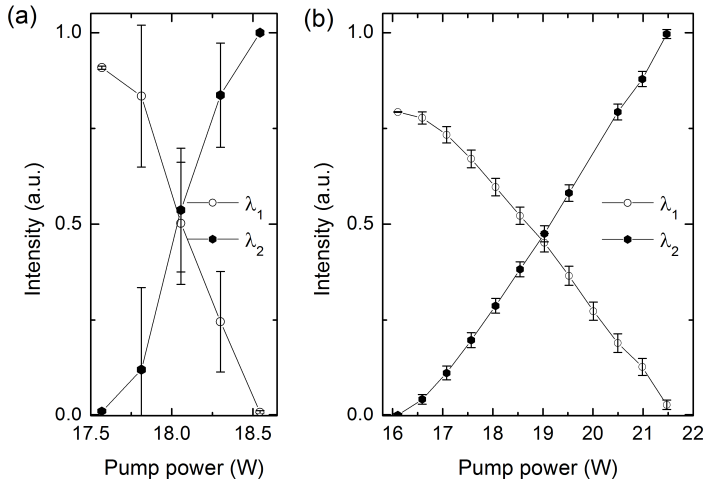

Figure 9: Operational ranges for stable 2-color emission in terms of pump power for (a) V-cavity and (b) F-cavity. Error bars indicate the magnitude of the noise behavior shown in Fig. 8

cavity is less sensitive fluctuations in operational parameters.

3.4 2-Color Discussion

The increased stability of 2-color operation in the F-cavity can be attributed to the increased complexity of the standing wave pattern formed within the gain region. Whereas the V-cavity we employ for comparison should have a fairly standard Gaussian distribution within the gain, the multiple interactions under two different angles in the F-cavity

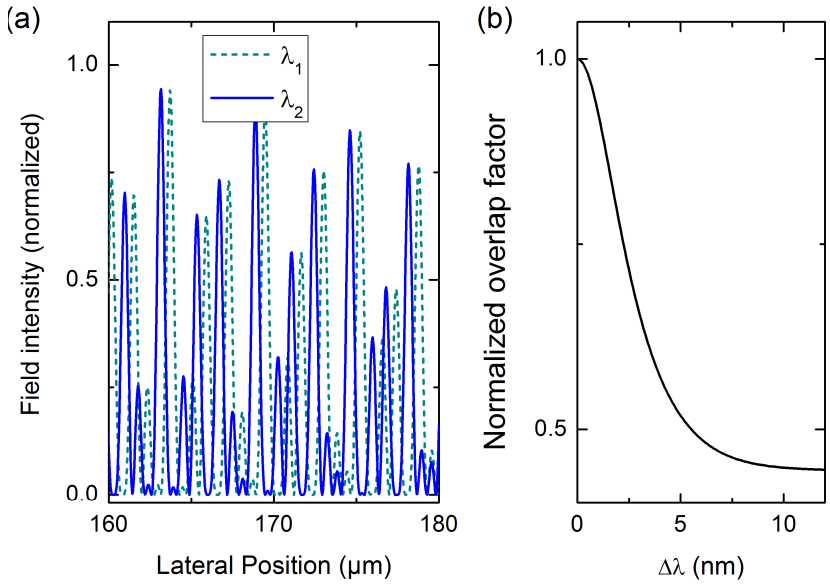

Figure 10: (a)Cross section of a simulated interference pattern for an F-cavity's intracavity field within the gain spot. (b)Plot of the overlap factor for two interference distributions based on their wavelength separation.

provide an interference pattern with sharp intensity spikes.

A cross section of a simple simulation of this interference patter is shown in Fig. 10a. Taking care to note that the cross section is pictured beginning 150 μm from the center of the overall gain spot (the spot is 420 μm diameter), one can see that the position of the interference fringes shifts dramatically with wavelength. Because each wavelength can only burn a hole where it has field intensity, the partial decoupling of the modes due to this fringe spacing helps alleviate the overall competition between the two modes, resulting in overall more stable coexistence of both lasing wavelengths. Fig. 10b presents an overlap factor defined by

$$\frac{\int_{-\infty}^{\infty} I_{\lambda 1}(x) * I_{\lambda 2}(x)\, dx}{\sqrt{\int_{-\infty}^{\infty} I_{\lambda 1}(x) * I_{\lambda 1}(x)\, dx * \int_{-\infty}^{\infty} I_{\lambda 2}(x) * I_{\lambda 2}(x)\, dx}}$$

where $I_{\lambda 1}(x)$ and $I_{\lambda 2}(x)$ define the respective intensities of fields for each wavelength (both wavelengths are assumed to be equal in power). The overlap factor quickly approaches a minimum value for a wavelength spacing of more than a couple nanometers, suggesting that this technique would be useful in inducing stable 2-color operation for a large variety of wavelength spacings in potential future 2-color VECSELs.

4. CONCLUSION

In conclusion, we have presented a novel cavity design expanding the idea of a multi-pass cavity to include passes under different angles. We have shown two particularly unique properties: that the blue-shift of the GDD profile can assist in the control of the net, round-trip GDD and that the complex interference pattern formed by the intracavity field supports highly stable 2-color operation by reducing the overlap of those two wavelengths' spatial distributions in the gain. We demonstrate the promise of these properties by presenting, first, record peak powers of 6.3 kW from a modelocked VECSEL, and second, 2.6W of highly stable emission on two wavelengths separated by 3nm.

ACKNOWLEDGEMENTS

This work is supported by the Air Force Office of Scientific Research (AFOSR) (BRI FA9550-14-1 -0062).

REFERENCES

[1] T.-L. Wang, B. Heinen, J. Hader, C. Dineen, M. Sparenberg, A. Weber, B. Kunert,S.W. Koch, J.V. Moloney, M. Koch, W. Stolz, "Quantum design strategy pushes high-power vertical-external-cavity surface-emitting lasers beyond 100 W." Laser & Photonics Reviews 6.5, L12-L14 (2012).

[2] J.E. Hastie, L. G. Morton, A. J. Kemp, M. D. Dawson, A. B. Krysa, and J. S. Roberts, "Tunable ultraviolet output from an intracavity frequency-doubled red vertical-external-cavity surface-emitting laser," Appl. Phys. Lett. 89, 061114 (2006)

[3] S. Kaspar, M. Rattunde, T. Töpper, R. Moser, S. Adler, C. Manz, K. Köhler, J. Wagner, Recent Advances in 2-\(\mu\)m GaSb-Based Semiconductor Disk Laser—Power Scaling, Narrow-Linewidth and Short-Pulse Operation," in IEEE Journal of Selected Topics in Quantum Electronics, 19, 1501908-1501908,(2013)

[4] Laurain, A., Mart, C., Hader, J., Moloney, J. V., Kunert, B., & Stolz, W. (2014). 15 W single frequency optically pumped semiconductor laser with sub-megahertz linewidth. IEEE Photonics Technology Letters, 26(2), 131-133.

[5] O. Casel, D. Woll, M. A. Tremont, H. Fuchs, R. Wallenstein, E. Gerster, P. Unger, M. Zorn, and M. Weyers, "Blue 489-nm picosecond pulses generated by intracavity frequency doubling in a passively mode-locked optically pumped semiconductor disk laser," Appl. Phys. B Lasers Opt., vol. 81, no. 4, pp. 443–446, 2005.

[6] D. Waldburger, S. M. Link, M. Mangold, C. G. E. Alfieri, E. Gini, M. Golling, B. W. Tilma, and U. Keller, "High-power 100 fs semiconductor disk lasers," Optica, vol. 3, no. 8, (2016)

[7] K.G. Wilcox, A.C. Tropper, H.E. Beere, D.A. Ritchie, B. Kunert, B. Heinen, and W. Stolz, "4.35 kW peak power femtosecond pulse mode-locked VECSEL for supercontinuum generation," Opt. Express 21, 1599-1605 (2013)

[8] M. Scheller, T.-L. Wang, B. Kunert, W. Stolz, S.W. Koch, J.V. Moloney, "Passively modelocked VECSEL emitting 682 fs pulses with 5.1 W of average output power," Electronics Letters,48, 588 – 589 (2012)

[9] M. Scheller, S. W. Koch, and J. V. Moloney, "Grating based wavelength control of single- and two-color vertical-external-cavity-surface-emitting lasers," Opt. Lett. 37, 25-27 (2012).

[10] M. Scheller, C. W. Baker, S. W. Koch and J. V. Moloney, "Dual-Wavelength Passively Mode-Locked Semiconductor Disk Laser," in IEEE Photonics Technology Letters, vol. 28, no. 12, pp. 1325-1327, June15, 15 2016.

[11] C. A. Zaugg, M. Hoffmann, W. P. Pallmann, V. J. Wittwer, O. D. Sieber, M. Mangold, M. Golling, K. J. Weingarten, B. W. Tilma, T. Südmeyer, and U. Keller, "Low repetition rate SESAM modelocked VECSEL using an extendable active multipass-cavity approach," Opt. Express 20, 27915-27921 (2012)

[12] M. Butkus, E. A. Viktorov, T. Erneux, C. J. Hamilton, G. Maker, G. P. A. Malcolm, and E. U. Rafailov, "85.7 MHz repetition rate mode-locked semiconductor disk laser: fundamental and soliton bound states," Opt. Express, vol. 21, no. 21, pp. 25526–25531, 2013.

[13] Kilen, I., Koch, S. W., Hader, J., & Moloney, J. V. (2016). Fully microscopic modeling of mode locking in microcavity lasers. JOSA B, 33(1), 75-80.

[14] Alexandre Laurain, Declan Marah, Robert Rockmore, John McInerney, Jorg Hader, Antje Ruiz Perez, Wolfgang Stolz, and Jerome V. Moloney, "Colliding pulse mode locking of vertical-external-cavity surface-emitting laser," Optica 3, 781-784 (2016)

[15] P. Klopp, U. Griebner, M. Zorn, and M. Weyers, "Pulse repetition rate up to 92 GHz or pulse duration shorter than 110 fs from a mode-locked semiconductor disk laser," Appl. Phys. Lett., vol. 98, no. 7, (2011)

[16] J. Hader, T. L. Wang, J. V. Moloney, B. Heinen, M. Koch, S. W. Koch, B. Kunert, and W. Stolz, "On the measurement of the thermal impedance in vertical-external-cavity surface-emitting lasers," J. Appl. Phys., vol. 113, no. 15, (2013)

[17] A. Bäumner, S. W. Koch, J. V. Moloney, "Non-equilibrium analysis of the two-color operation in semiconductor quantum-well lasers," physica status solidi (b) 248, 843–846 (2011).

[18] A. Chernikov, M. Wichmann, M. K. Shakfa, M. Scheller, J. V. Moloney, S. W. Koch, and M. Koch, "Time-dynamics of the two-color emission from vertical-external-cavity surface-emitting lasers," Appl. Phys. Lett. 100, 041114 (2012)

[19] F. Zhang, M. Gaafar, C. Möller, W. Stolz, M. Koch, A.Rahimi-Iman, "Dual-Wavelength Emission From a Serially Connected Two-Chip VECSEL", IEEE Photonics Technology Letters, 28, 927-929 (2016)